

Dispelling Dampness, Relieving Turbidity and Dredging Collaterals Decoction, Attenuates Potassium Oxonate-Induced Hyperuricemia in Rat Models

Hai-bo Liu^{1,*}, Min Yang^{2,*}, Wan Li², Ting Luo², Yang Wu², Xiang-yu Huang², Yao-lei Zhang³, Tao Liu², Yong Luo^{2,*}

¹Department of Biomedical Engineer, General Hospital of Western Theater Command, Chengdu, Sichuan, People's Republic of China; ²Department of Traditional Chinese Medicine, General Hospital of Western Theater Command, Chengdu, Sichuan, People's Republic of China; ³Basic Medical Laboratory, General Hospital of Western Theater Command, Chengdu, Sichuan, People's Republic of China

*These authors contributed equally to this work

Correspondence: Yong Luo, Department of Traditional Chinese Medicine, General Hospital of Western Theater Command, Chengdu, Sichuan, 610083, People's Republic of China, Tel +86 28-86571619, Email yongl019@sina.com

Purpose: Dispelling dampness, relieving turbidity and dredging collaterals decoction (DED), is a traditional Chinese medicine used in the treatment of hyperuricemia. We aimed to explore the effect and mechanism of DED in the treatment of hyperuricemia.

Methods: The effects of DED (9.48, 4.74, and 2.37 g/kg/d) on potassium oxonate (750 mg/kg/d)-induced hyperuricemia in rats were evaluated by serum uric acid (UA), creatinine (CRE), blood urea nitrogen (BUN), and renal pathological changes. Network pharmacology was used to identify the effective components and targets of DED, and the key targets and signaling pathways for its effects on hyperuricemia were screened. Molecular docking was used to predict the action of DED. H&E, immunohistochemistry, WB, and PCR were used to validate the network pharmacology results.

Results: DED can effectively alleviate hyperuricemia, inhibit UA, CRE, BUN, and xanthine oxidase (XOD) activity, and reduce renal inflammatory cell infiltration and glomerular atrophy. The experiment identified 27 potential targets of DED for hyperuricemia, involving 9 components: wogonin, stigmasterol 3-O-beta-D-glucopyranoside, 3β-acetoxyatractylone, beta-sitosterol, stigmasterol, diosgenin, naringenin, astilbin, and quercetin. DED can relieve hyperuricemia mainly by inhibiting RAGE, HMGB1, IL17R, and phospho-TAK1, and by regulating the AGE-RAGE and IL-17 signaling pathways.

Conclusion: DED can alleviate hyperuricemia by inhibiting XOD activity and suppressing renal cell apoptosis and inflammation via the AGE-RAGE signaling pathway and IL-17 signaling pathway. This study provides a theoretical basis for the clinical application of DED.

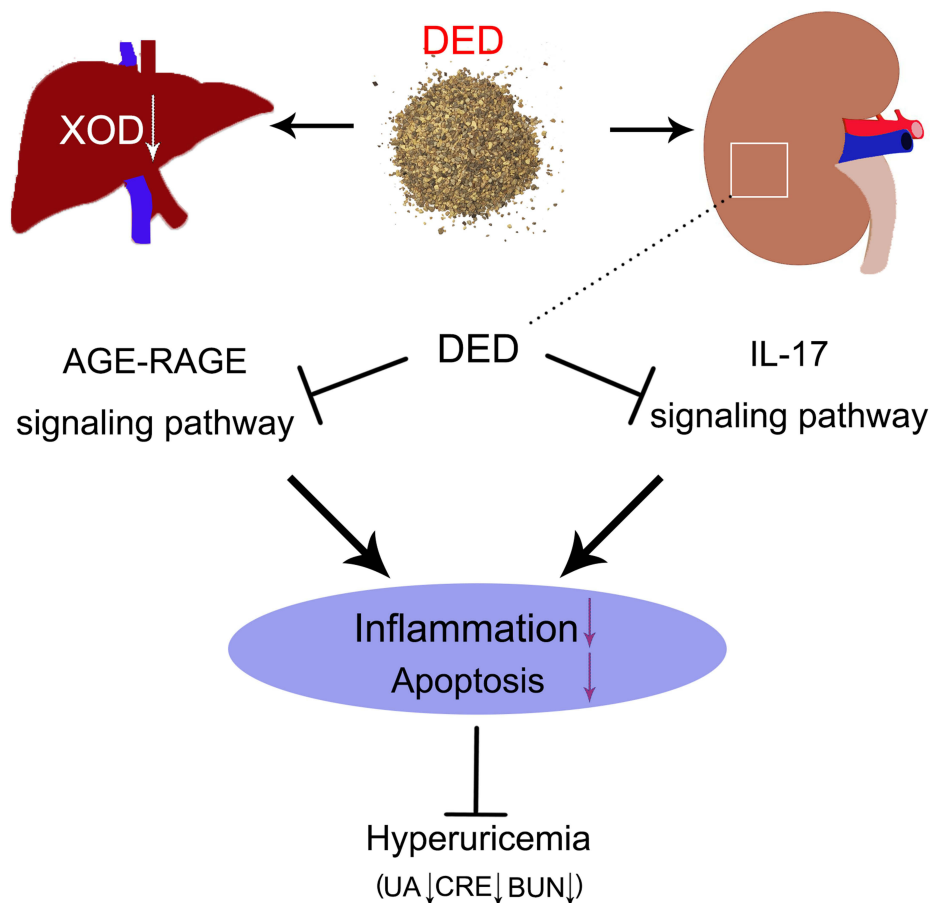
Keywords: dispelling dampness, relieving turbidity, dredging collaterals, hyperuricemia, network pharmacology

Introduction

Hyperuricemia is an independent risk factor for diseases such as gout, chronic kidney disease, hypertension, cardiovascular and cerebrovascular diseases, and diabetes; and is also an independent predictor of premature death. Hyperuricemia is caused by purine metabolism disorders,¹ characterized by elevated serum uric acid levels. Although commonly used urate-lowering drugs such as allopurinol, febuxostat, and benzbromarone have some effectiveness, their long-term use leads to significant adverse effects.^{2,3} Therefore, finding a safe and effective drug is urgent.

Studies have proven that hyperuricemia is a systemic disease that can induce renal inflammation by activating NLRP3, promote cardiomyocyte apoptosis through ROS expression upregulation, and regulate TGF-β pathways to promote cell autophagy.^{4,5} According to the theory of traditional Chinese medicine, “dispelling dampness, relieving turbidity and dredging collaterals” are the basic treatment principles of hyperuricemia renal injury.^{6,7} “Dispelling dampness, relieving turbidity and

Graphical Abstract



dredging collaterals decoction (DED)" consists of *yam rhizome*, *rhizoma smilacis glabrae*, *cortex phellodendri*, *Atractylodis rhizoma*, *medicinal cyathula root*, *semen coicis*, and *Ligusticum wallichii*. *Atractylodis rhizoma* and *semen coicis* contain various anti-inflammatory and anti-apoptotic ingredients that are used to dispel dampness.^{8,9} The *yam rhizome*, *rhizoma smilacis glabrae* and *cortex phellodendri* play a significant role in regulating uric acid transporters and glucose transporters in renal tubules¹⁰⁻¹² and are used to relieve turbidity. *Magnograndiolide* is the main component of medicinal cyathula root and *Ligusticum wallichii* in promoting blood circulation and removal of blood stasis and has anti-inflammatory, antioxidant and antifibrosis effects¹³ used for promoting dredging collaterals. The above drugs are used together to relieve hyperuricemia. The mechanism is still unclear due to the characteristics of multicomponent and multitarget DED.

Due to the complex nature of the ingredients and mechanisms of DED, it is difficult to reflect the systematic effect of DED on hyperuricemia through research on a single component or target. This study used network pharmacology and molecular docking to screen for the potential pharmacological components and targets of compounds.^{14,15} Network pharmacology plays an important role in elucidating the therapeutic mechanisms of traditional Chinese medicine, especially for the targeting characteristics of the multiple pathways of traditional Chinese medicine, and combined with animal model verification, it elucidates the mechanism of DED in hyperuricemia treatment.

Materials and Methods

Drug Target Screening

Inquiry through TCMSP database (<http://tcmsp.com/tcmssp.php>) to eliminate the in DED with seven kinds of Chinese medicine effective active ingredient and targets. Hyperuricemia disease related targets through DisGeNET (<https://www.disgenet.org/>) to

query the Database. Use Venny 2.1 database (<https://bioinfo.gp.cnb.csic.es/tools/venny/>) to remove the DED and hyperuricemia hematic disease targets for overlay analysis.

Protein-Protein Interaction (PPI) Network

The overlapping genes were introduced (<https://string-db.org/>) to construct PPI model, and Cytoscape3.9.1 was used for visualization.

Component-Target-Disease Network

Component, target, and disease were introduced into Cytoscape3.9.1 to construct a composite target network, and the relationships among them were analyzed by visualization processing.

Gene Ontology (GO) and Pathway Enrichment

Overlap the role of the relationship between targets and pathways, by DAVID2021 (<https://david.ncifcrf.gov/>). The target was imported into DAVID for GO analysis and KEGG path analysis, and visualization was carried out.

Molecular Docking

In order to further understand the binding ability of key targets and compounds in DED, we have interacted with key compounds and targets in DED through molecular docking. The three-dimensional (3D) structure of the compound is first obtained from ChemDraw, and its energy is minimized by ChemOffice software. The receptor 3D structure was obtained from the PDB database (<https://www.rcsb.org/>). After residue removal, deoxidation and hydrotreatment by PyMOL software, AutoDockTools 1.5.6 software converted the format of receptor and ligand into PDBQT, AutoDock Vina platform simulated the selected target, and selected the conformation with the best binding affinity as the final docking conformation. The visualization was carried out by PyMOL software.

DED Preparation

DED was composed of 30 g *yam rhizome*, 30 g *rhizoma smilacis glabrae*, 15 g *cortex phellodendri*, 20 g *Atractylodis rhizoma*, 30 g *medicinal cyathula root*, 30 g *semen coicis*, and 15 g *Ligusticum wallichii*. All reagents were purchased from the Pharmacy of Traditional Chinese Medicine, Western Theater Command General Hospital (Chengdu, China). Add distilled water and boil for 1.5 h under 0.08 MPa pressure, repeated 3 times. Filter the extract under reduced pressure and concentrate it to a relative density of 1.0–1.2. After vacuum drying, the sample was ground into a fine powder.

Establishment of the Animal Model

The study was approved by the Animal Research Ethics Committee of The General Hospital of Western Theater Command (Chengdu, China) and complied with the Guidelines for Animal Experiments (Ethical approval number: 2022EC2-007). Forty-eight male SD rats at 6 weeks of age and weighing 180–200 g were purchased from Chengdu Dashuo Biotechnology Co., Ltd. (China; license no. SCXK 2015–030). All rats were maintained on a 12/12-h light dark cycle, were allowed free access to water and food, and were acclimated for at least 7 days prior to surgery.

Hyperuricemia was induced in rats by potassium oxazinate (PO) intragastric administration.¹⁶ The model method was as follows: except for the control group, which was given the same amount of normal saline by intragastric administration, the other groups were given 750 mg/kg/d PO by intragastric administration once a day for 14 consecutive days.¹⁶ All male rats were divided into six groups: control group (control, n=8), hyperuricemia model group (HU, n=8), low-dose group (DED-L, n=8), medium-dose group (DED-M, n=8), high-dose group (DED-H, n=8) and benzbromarone (BBR, n=8) group. The drug volume of the treatment group was 10 mL/kg, and the dose was 9.48 g/kg/d in the high-dose group, 4.74 g/kg/d in the medium-dose group, and 2.37 g/kg/d in the low-dose group. The control group and model group were given the same amount of normal saline by intragastric administration. The BBR group was given BBR intragastrically at 1 mg/kg/d. The drug was administered once daily for 14 days. After administration, all rats fasted for 12 h and were

anesthetized with 3% pentobarbital sodium, and then blood was removed to separate the serum. Kidney tissue samples were collected and stored at -80°C and 4% paraformaldehyde (BL539A, Biosharp, China) for further testing.

H&E Staining

The kidney tissues of rats in each group were fixed with 4% paraformaldehyde, and 6 sections ($4\ \mu\text{m}$) were randomly selected for routine H&E (BL700B, Biosharp, China) staining. The morphological changes in kidney tissues were observed by ordinary light microscopy (DM3000, Leica, GER).

Detection of Serum Hyperuricemia-Related Indicators

Serum uric acid (BC1365, Solarbio, China), serum creatinine (BC4915, Solarbio, China), and blood urea nitrogen (BC1535, Solarbio, China) were prepared according to the reagent instructions (Multiskan GO, Thermo, USA) to determine the absorbance of each sample.

Determination of Xanthine Oxidase Activity

Rat liver tissue (1.0 g) was weighed and added to precooled normal saline at a ratio of weight (mg) to volume (μL)=1:10. The liver homogenate was prepared by mechanical homogenization in an ice water bath at low temperature. The liver homogenate was centrifuged at 3500 rpm/min for 10 min (4°C), and the supernatant was obtained. Xanthine oxidase activity was determined using an XOD kit (BC1095, Solarbio, China). Ten microliters of tissue homogenate supernatant and serum were added to 40 μL of hypoxanthine and 40 μL of hydroxylamine hydrochloride and incubated at 37°C for 20 min. Then, 60 μL of 4-aminobenzenesulfonamide and 60 μL of N-(1-naphthyl)-ethylenediamine were added and incubated at 37°C for 20 min. The absorbance value was measured at 530 nm. The xanthine oxidase activity of the sample to be detected was calculated by determining the standard (sodium nitrite) and blank absorbance.

Western Blot

The total protein of each group was extracted by a protein extraction kit (KGP250, KeyGEN, China) and quantified by a protein quantification kit (KGP902, KeyGEN, China). The protein sample size was 20 μg . The total protein was obtained by SDS-PAGE (P1200, Solarbio, China), and the protein was transferred to solid-phase carrier PVDF membrane (IPFL00010, Millipore, Germany), and the primary antibody was added: anti-RAGE (ab216329, abcam, UK), anti-HMGB1 (6893, CST, USA), anti-IL-17RA (bs-2606R, Bioss, China), anti-TAK1 (ab109526, abcam, UK), anti-Phospho-TAK1 (bs-5435R, Bioss, China), anti- β -actin (bs-0061R, Bioss, China), incubated overnight at 4°C , added secondary antibody: Goat anti-rabbit (bs-0295G, Bioss, China), Goat anti-mouse (bs-0296G, Bioss, China), incubated at room temperature for 40 min and added substrate (WBKLS0100, Millipore, Germany), developed by chemiluminescent image (A300, Azrue, USA).

Real-Time Quantitative PCR

Total RNA was extracted by TRIzol (155596-026, Thermo, USA). Subsequent experiments were conducted with a total RNA purity between 1.8 and 2.0 (260 nm/280 nm), and cDNA was obtained by a reverse transcription kit (RR047A, TAKARA, Japan). Two microliters of cDNA was added to 2.5 μL SYBR premix Ex Taq, 1.0 μL forward primer (Table 1), 1.0 μL reverse primer (Table 1), and 8.5 μL RNase Free dH_2O and mixed thoroughly. According to the RT-qPCR kit (RR820A, TAKARA, Japan) manufacturer's instructions, the initial step was 95°C for 30s, followed by 40 cycles of 95°C for 5 s and 60°C for 30s. Gene expression was detected by fluorescence quantitative RT-qPCR (CFX96, Biorad, USA). Relative gene expression was calculated by using the $\Delta\Delta\text{Ct}$ method using the Equation $2^{-\Delta\Delta\text{Ct}}$, with GAPDH as an internal quantitative control.

Immunohistochemistry

The tissues were dehydrated and embedded, sliced ($4\ \mu\text{m}$), dewaxed and rehydrated, then placed in 100°C acid repair solution (BL619A, Biosharp, China) for 2 min, and blocked with endogenous peroxidase by 3% H_2O_2 , and incubated with goat serum (AR1009, BOSTER, China) for 10 min. The following antibodies were added: anti-IL-6 (bs-4539R,

Table 1 Primers Which Have Been Used for RT-qPCR

Primer Name	Sequence 5'-3'	Product Length
RAGE	Forward: GTCCAACTACCGAGTCCGAGTCTAC Reverse: GCCTCCTGGTCTCCTCCTTCAC	209 bp
HMGB1	Forward: GCCCATTTTGGGTACATGG Reverse: TGCAGGGTGTGTGGACAAAA	76 bp
IL17R	Forward: ATCTTGCCAACAACAGACCTGACTC Reverse: GACGATGATCTTGAACCGCTCTC	246 bp
TAK1	Forward: CGCCATCGCAGGTCCTTAACTTC Reverse: GCCTCCTTCAGCATACTCCATCAC	269 bp
GAPDH	Forward: AGTGCCAGCCTCGTCTCATA Reverse: GGTAACCAGGCGTCCGATAC	77 bp

Bioss, China), anti-Caspase-8 (bsm-33190 M, Bioss, China), and anti-IL-1 β (bs-0812R, Bioss, China). The samples were incubated at 4 °C overnight, and the protein localization and expression were detected by an immunohistochemical kit (PV9000, ZSGB, China). The changes in protein expression in renal tissue were observed by ordinary optical microscopy ($\times 200$), and the density of each group was calculated by Image-Pro Plus (IPP).

Statistical Analysis

SPSS 25.0 software was used for statistical analysis of the experimental data. For normally distributed data, one-way ANOVA or unpaired two-tailed Student's *t*-test was used to determine the differences among groups. For nonnormally distributed data, the Kruskal–Wallis test was used. All the data are expressed as the mean \pm standard deviation. Statistically significant differences were considered significant at $p = 0.05$, * $p < 0.05$, ** $p < 0.01$, and *** $p < 0.001$.

Results

Effective Ingredients of DED

We screened the effective ingredients and target points of DED, and the results showed that DED contains 72 effective ingredients and has 245 and 196 target points for hyperuricemia and DED, respectively. Among them, 27 potential target points for DED in hyperuricemia corresponded to 9 effective ingredients (Figure 1A). The PPI network represents the interactions among the target points. The 27 target nodes related to 184 edges, with an average node degree of 13.6 and an average local clustering coefficient of 0.81. The PPI enrichment *P* value was less than 1.0×10^{-16} (Figure 1B). The top 10 hub genes included IL6, TNF, CCL2, VEGFA, MAPK3, IL1B, CASP3, PPARG, CAT, and IL10. The darker and larger the node's color, the more critical the protein may be in the treatment of hyperuricemia (Figure 1C). These results suggest that these proteins may be more crucial in the treatment of hyperuricemia with DED.

DED Alleviates Hyperuricemia in Rats

The effect of DED on hyperuricemic nephropathy was explored by HE staining. The results showed that compared with the control group (Figure 2A), the model group (Figure 2B) had local inflammation, cytoplasmic vacuoles and dilation, and partial glomerular atrophy in renal tissues. Compared with the model group, the low, medium, and high doses of DED and the BBR group (Figure 2C–F) all improved renal damage, with the medium dosage obtaining a significant effect, mainly manifested as smaller inflammatory lesions and significant relief of glomerular atrophy. The serum levels of UA, CRE, and BUN are important indicators of renal function changes. The results showed that compared to the control group, the model group had significantly increased levels of UA, CRE, and BUN ($p < 0.001$), while the medium and high doses of DED significantly reduced the levels of these substances in the blood ($p < 0.05$) (Figure 2G–I). Low-dose DED had no significant effect on adjusting BUN ($p > 0.05$). The results suggest that DED can effectively alleviate hyperuricemia, yet the target site of action remains unclear.

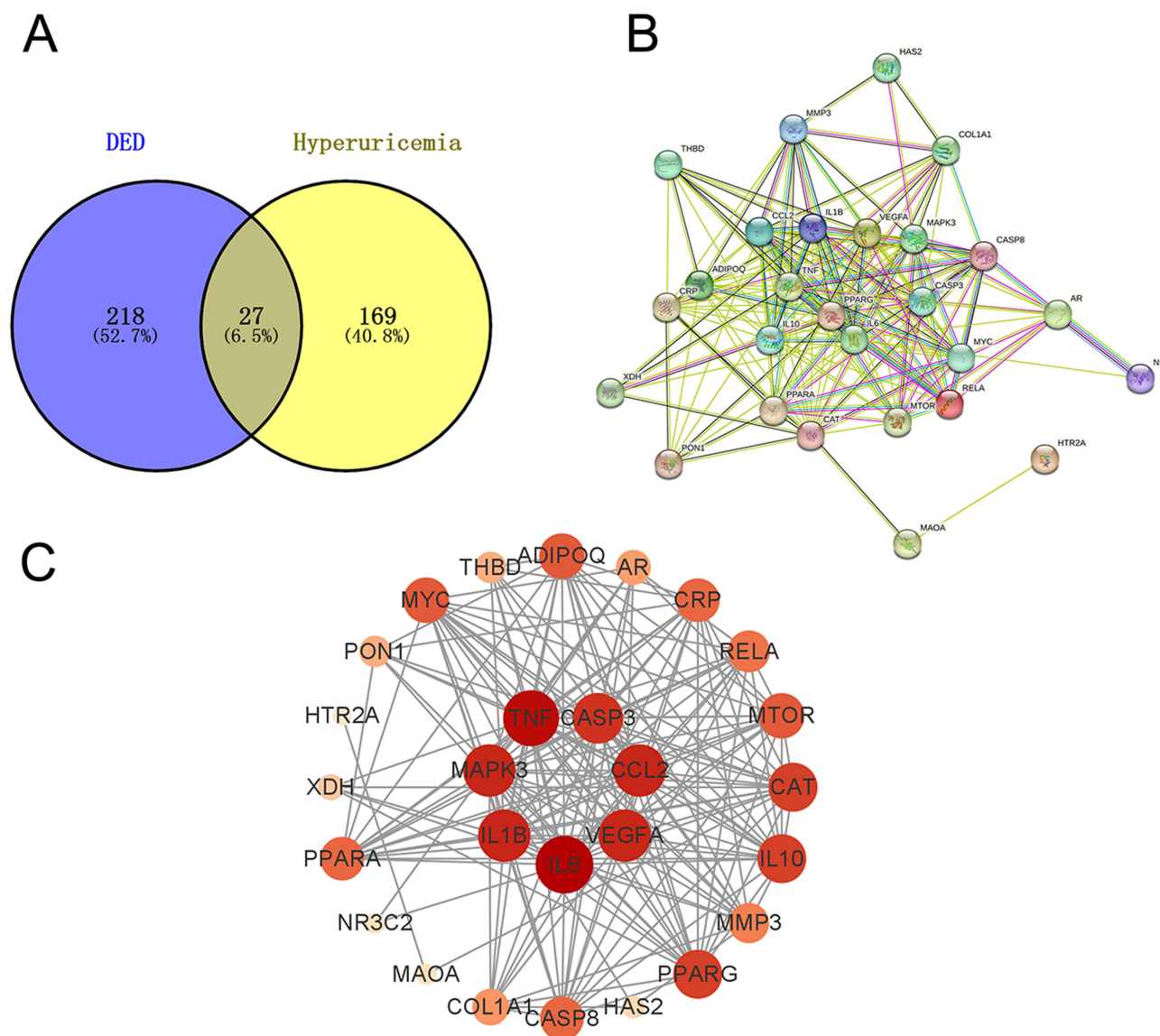


Figure 1 Key targets and interaction network of the drug. The overlapping gene targets between DED and hyperuricemia (**A**). The interaction relationships between corresponding proteins of the targets and the differentiation of the importance of targets (**B** and **C**).

Network Analysis of the Effect of DED on Hyperuricemia

Network pharmacology has significant advantages in analyzing the targets of traditional Chinese medicine formulas for disease.¹⁷ Twenty-seven potential targets were analyzed using the DAVID database, resulting in 176 GO entries, including 145 biological processes (BP), 10 cell compositions (CC), and 21 molecular functions (MF). The top 10 entries of BP, CC, and MF were selected based on the P value, and a graph was drawn using the GraphPad (Figure 3A). BP mainly includes positive regulation of gene expression, positive regulation of pri-miRNA transcription from the RNA polymerase II promoter, response to activity, etc.; CC mainly includes extracellular space, extracellular region, and macromolecular complex, etc.; MF mainly includes identical protein binding, cytokine activity, macromolecular complex binding, etc.

Based on the component-target-disease analysis, we created a network of 17 KEGG pathways for DED. The results showed that there were 10 KEGG pathways shared between DED and hyperuricemia, indicating that they have common targets for anti-hyperuricemia. Network pharmacology revealed the importance of IL6, TNF, CCL2, VEGFA, MAPK3, IL1B, CASP3, PPARG, CAT, and IL10. Therefore, DED may mainly alleviate cell apoptosis and the immune response through the AGE-RAGE signaling pathway and IL-17 signaling pathway and work together with other pathways to alleviate hyperuricemia (Figure 3B).

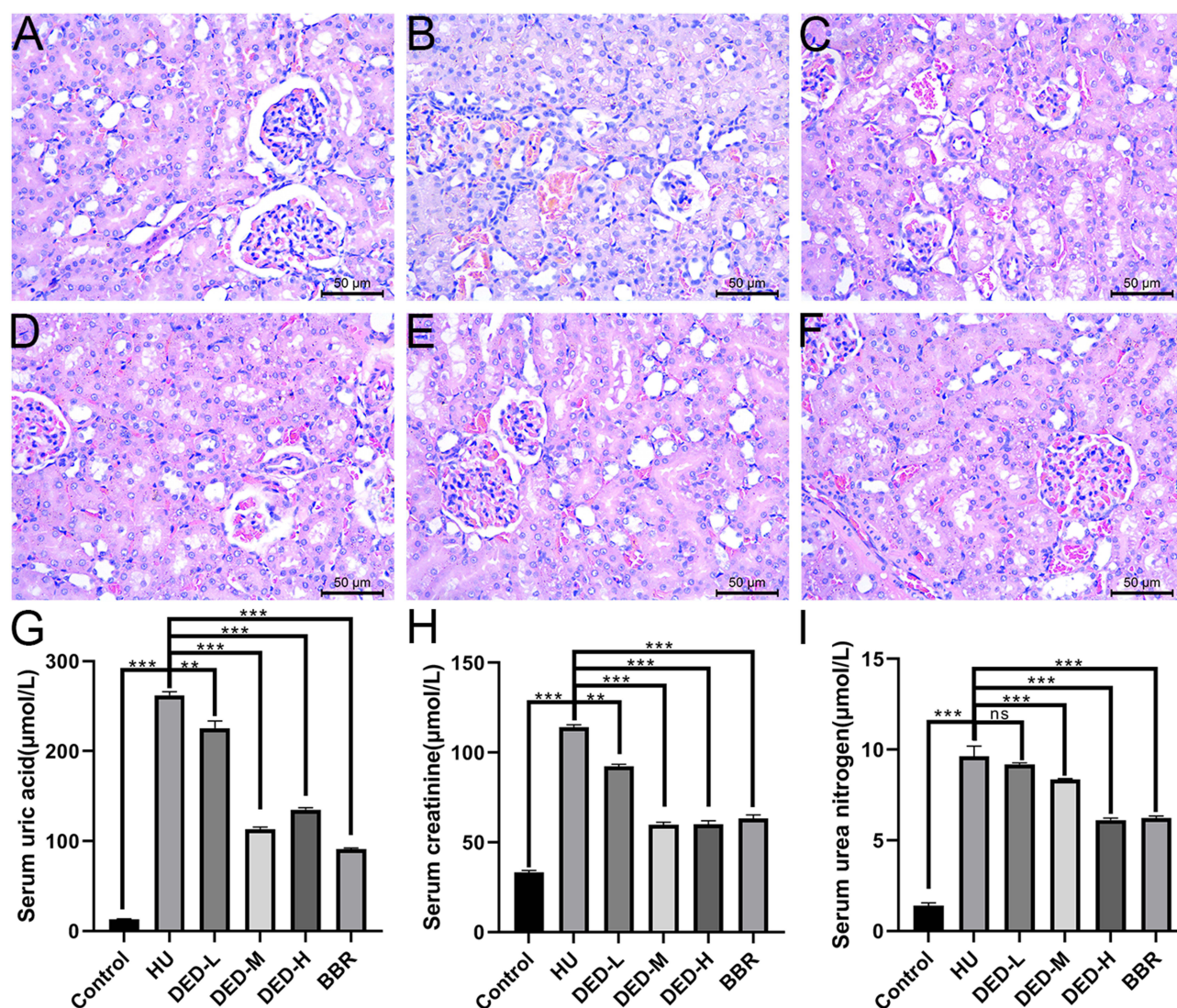


Figure 2 Histological changes in the kidney structure. (A) Control group. (B) Model group. (C) DED low-dose group. (D) DED medium-dose group. (E) DED high-dose group. (F) BBR group. (G) Changes in serum UA levels in each group. (H) Changes in serum CRE levels in each group. (I) Changes in serum BUN levels in each group. The data in each group of eight rats are presented as the mean \pm standard deviation (\pm S). *** $p < 0.001$; ** $p < 0.01$; ns $p > 0.05$.

Molecular Dock

Molecular docking analysis was conducted to investigate the binding between the key components of DED and the key targets. Typically, ligand–receptor pairs with low energy binding conformational stability are more likely to interact. The results showed that the key targets TNF, VEGF, and IL6, bonded well with all key components, and their binding free energy was relatively low, ranging from -6.2 to -9.0 kcal/mol (Table 2). Among them, TNF had the lowest energy with stigmasterol (-7.3 kcal/mol), VEGF had the lowest energy with diosgenin (-9.0 kcal/mol), and IL6 had the lowest energy with diosgenin (-7.8 kcal/mol). The visualization of molecular docking displayed the results of 9 pairs of molecular targets (Figure 4A–I), suggesting that DED may alleviate hyperuricemia by binding to multiple targets.

Effect of DED on Serum and Liver XOD Activity in Hyperuricemic Rats

XOD is a critical enzyme involved in the generation of uric acid. With comparison to the control group, the serum XOD activity level in the model group was significantly increased ($p < 0.001$). Compared to the model group, benzbromarone effectively inhibited serum and liver XOD activity. DED at medium ($p < 0.001$) and high ($p < 0.001$) doses effectively inhibited liver XOD activity, especially in the high-dose group, in which the downregulation was the largest. However,

Table 2 Binding Energy Between Selected Targets and Active Compounds

Molecule Name	Binding Energy (Kcal/Mol)		
	TNF	VEGFA	IL6
3 β -acetoxyatractylone	-6.6	-7.1	-6.2
Astilbin	-6.7	-7.7	-6.9
Beta-sitosterol	-6.3	-7.9	-7.0
Diosgenin	-7.3	-9.0	-7.8
Naringenin	-6.6	-7.3	-6.8
Quercetin	-6.8	-7.3	-6.7
Stigmasterol	-7.3	-8.6	-6.7
Stigmasterol 3-O-beta-D-glucopyranoside	-6.8	-7.8	-6.9
Wogonin	-7.0	-6.7	-6.4

with the molecular docking results, the experimental results suggest that DED may alleviate the progression of hyperuricemia by targeting the binding of IL-6, CASP-8, and IL-1 β .

DED Inhibits the AGE-RAGE Signaling Pathway

Through experimental validation of the enriched pathway results from network pharmacology, the results showed that compared to the control group, RAGE expression in the model group's kidney tissues was significantly increased ($p < 0.001$). Compared to the model group, the low ($p > 0.05$), middle ($p > 0.05$), high-dose ($p < 0.01$) and BBR groups ($p < 0.01$) of DED were able to downregulate RAGE expression, but only the high-dose and BBR groups had significant differences. Consistent with the expected results, potassium oxonate significantly promoted HMGB1 expression ($p < 0.001$). Compared to the model group, the low ($p > 0.05$), middle ($p < 0.01$), high-dose ($p < 0.001$), and BBR groups ($p < 0.01$) of DED were able to downregulate the expression of both RAGE and HMGB1, but only the middle- and high-dose

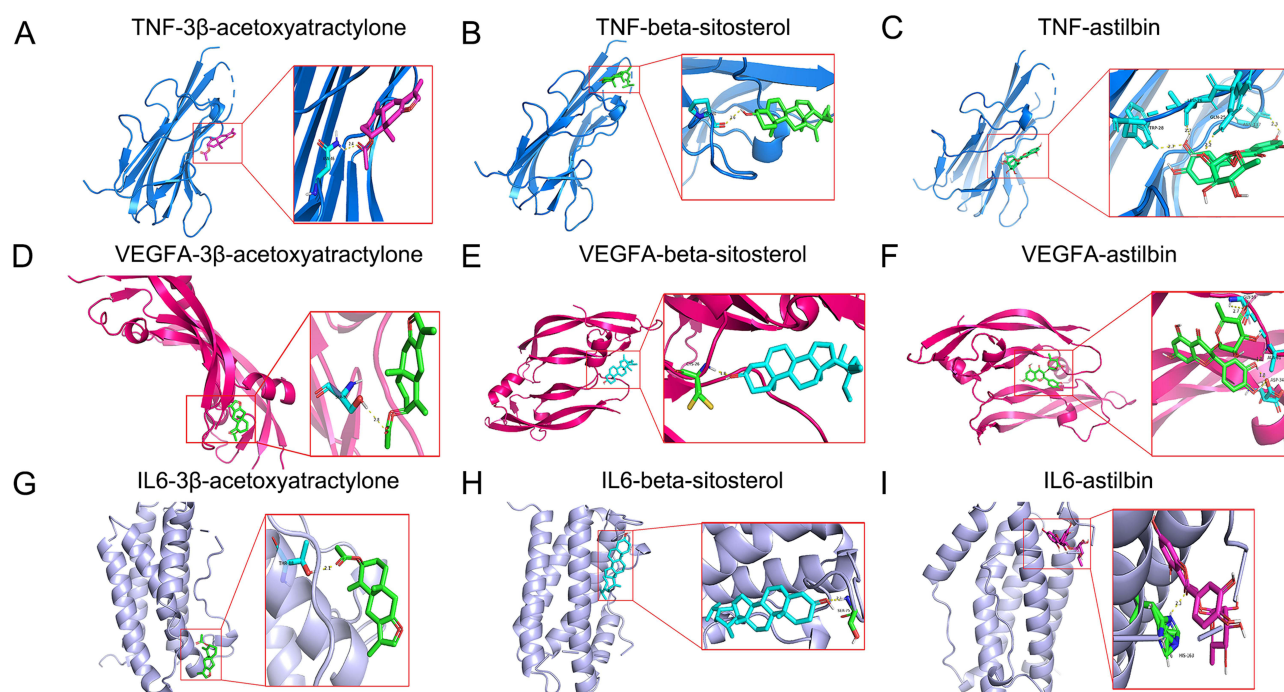


Figure 4 Molecular docking and visualization results. (A–C) Visual results of the docking between three key components and TNF. (D–F) Visual results of the docking between three key components and VEGF. (G–I) Visual results of the docking between three key components and IL6.

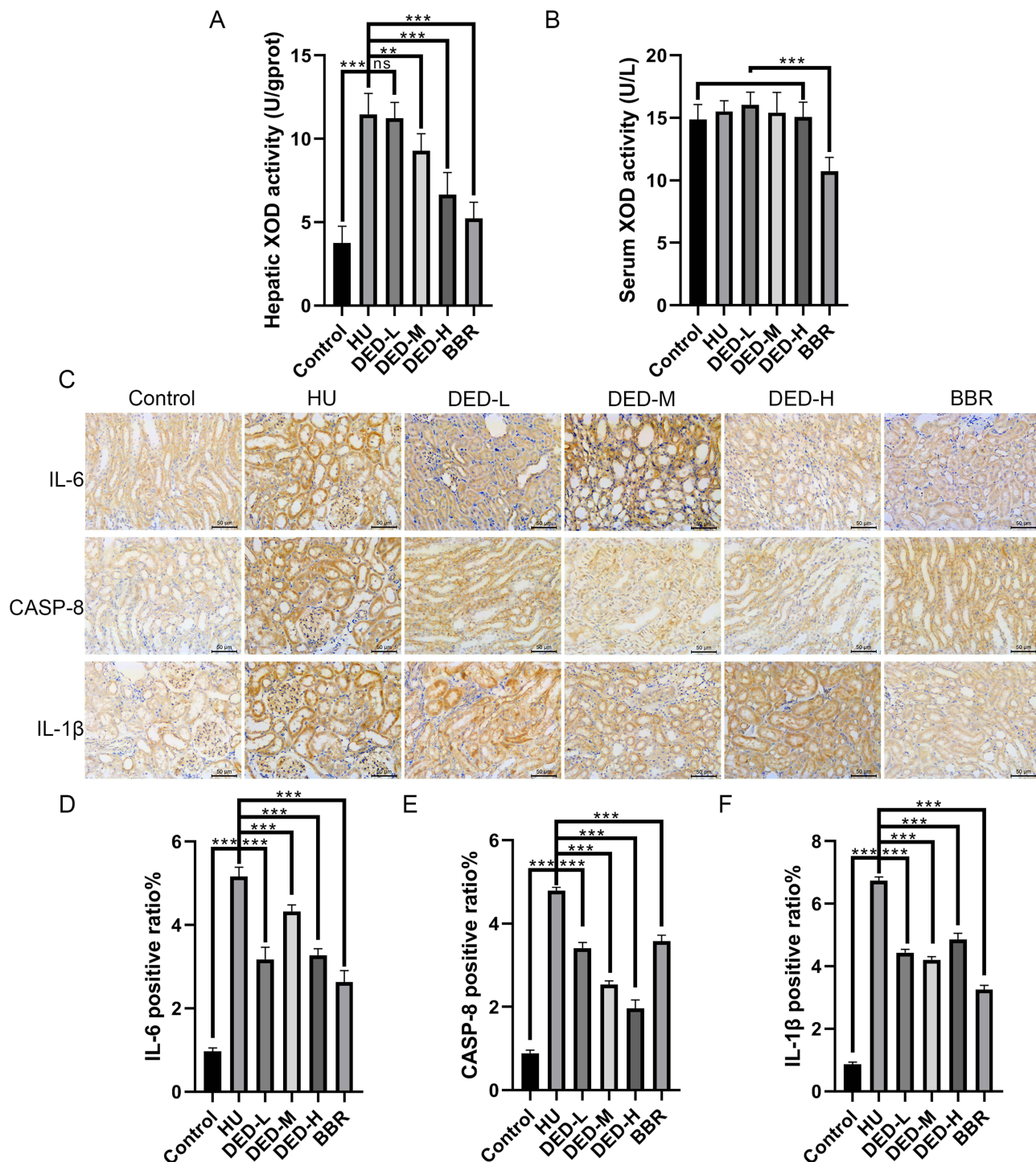


Figure 5 Molecular changes in XOD activity in serum and liver tissue of each group. (A) Changes in serum XOD activity. (B) Changes in liver XOD activity. (C) Immunohistochemistry was used to detect the expression of IL-6, CASP8, and IL-1 β in kidney tissue. (D) Statistical analysis of the mean optical density of IL-6. (E) Statistical analysis of the mean optical density of CASP-8. (F) Statistical analysis of the mean optical density of IL-1 β . The data are presented as the mean \pm standard deviation (\pm S) for each group of eight mice. *** $p < 0.001$; ** $p < 0.01$; * $p < 0.05$; ns $p > 0.05$.

groups and the BBR group had significant differences. The PCR results were consistent with the WB results, and DED significantly downregulated the expression of the RAGE and HMGB1 genes. These results suggest that DED may inhibit the activation of the AGE-RAGE signaling pathway and alleviate hyperuricemia (Figure 6A–C and G).

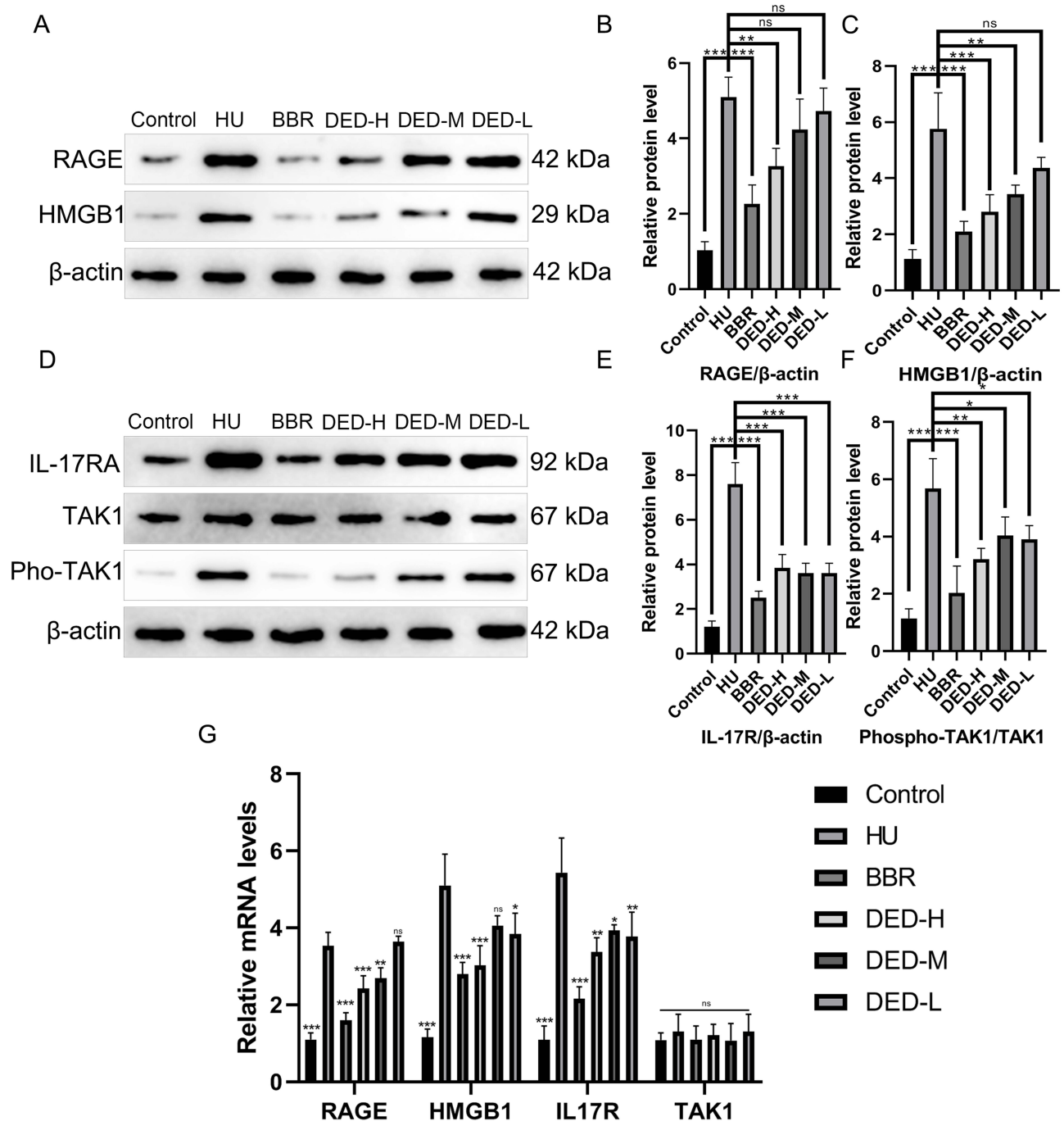


Figure 6 Changes in key proteins and gene expression of the AGE-RAGE and IL-17 signaling pathways. Western blotting was used to detect changes in the expression of the renal AGE-RAGE signaling pathway (A) and IL-17 signaling pathway (D) in each group. GAPDH was used as an internal reference protein, and the gray value of each protein expression was counted for RAGE (B), HMGB1 (C), IL-17R (E), and phospho-TAK1/TAK1 (F). (G) Changes in key gene expression. In each group of three rats, the data are expressed as the mean \pm standard deviation (\pm S). *** $p < 0.001$; ** $p < 0.01$; * $p < 0.05$; ns $p > 0.05$.

DED Inhibits the IL-17 Signaling Pathway

In the experiment, changes in the expression of another key signaling pathway protein and gene were simultaneously detected. The results showed that compared with the control group, the model group had significantly elevated IL17R expression in kidney tissue ($p < 0.001$), no significant difference in total TAK1 expression ($p > 0.05$), and increased phospho-TAK1 expression ($p < 0.01$). Compared with the model group, DED at low ($p < 0.001$), medium ($p < 0.001$), high-dose ($p < 0.001$), and BBR groups ($p < 0.001$) significantly downregulated IL17R expression; DED at low ($p <$

0.05), medium ($p < 0.05$), high-dose ($p < 0.01$), and BBR groups ($p < 0.001$) significantly downregulated phospho-TAK1 expression, blocking pathway activation. The PCR results were consistent with the WB results, showing that DED could significantly downregulate IL17R gene expression ($p < 0.05$), while TAK1 expression showed no significant differences ($p > 0.05$). These results suggest that DED may inhibit the activation of the IL-17 signaling pathway and alleviate hyperuricemia (Figure 6D–G).

Discussion

Based on multiple complications of hyperuricemia and side effects of existing drugs, there is an urgent need to find a new adjuvant medication. In this study, we found that DED can significantly reduce serum uric acid, CRE and BUN levels and downregulate XOD activity, thereby improving renal lesions caused by hyperuricemia. It was also found that DED may alleviate hyperuricemia by inhibiting the activation of the AGE-RAGE signaling pathway and IL-17 signaling pathway (Graphical Abstract).

Traditional Chinese medicine (TCM) is increasingly receiving attention worldwide, with an increasing number of traditional Chinese medicines being used as the clinical treatment of hyperuricemia.⁵ Studies have proven that hyperuricemia is directly related to uric acid metabolism disorder. Sodium urate crystal deposition is the main clinical manifestation of hyperuricemia, and XOD is the key rate-limiting enzyme involved in uric acid metabolism. High XOD activity can lead to excessive synthesis of UA.¹⁸ It has been shown that based on the principles of dispelling dampness, clearing turbidity, and promoting blood circulation, TCM can significantly alleviate hyperuricemia.¹⁹ This article combines dispelling dampness, relieving turbidity, and unblocking collaterals, and based on previous research,^{20,21} innovatively introduces the DED compound formula. As a whole Chinese herbal compound, many components and corresponding components of DED have been proven to alleviate hyperuricemia.^{6,8} In this study, the experimental results show that DED can inhibit XOD activity in the liver in PO-induced hyperuricemic rats and inhibit the inflammation and apoptosis of kidney cells, which is consistent with the conclusions of related studies.¹⁰ Surprisingly, DED did not affect serum XOD activity, possibly due to its inability to target all other tissues capable of producing XOD.²² The results suggest that the effect of DED on reducing uric acid is mainly to target liver XOD, inhibit its activity, and then inhibit the production of xanthine, thereby reducing uric acid production.

The levels of CRE and BUN are important biochemical indicators for detecting renal dysfunction.²³ This study found that DED can significantly reduce serum UA, CRE and BUN levels, suggesting that DED can alleviate hyperuricemia induced by potassium oxazinate, which may be a therapeutic strategy for renal injury. DED contains 9 effective components that correspond to the targets of hyperuricemia, including wogonin,²⁴ beta-sitosterol,²⁵ stigmasterol,²⁶ diosgenin,²⁷ naringenin,²⁸ astilbin,²⁹ and quercetin,³⁰ which have been shown to alleviate hyperuricemia. The results of this experiment also support these studies, as DED can improve renal tissue lesions by downregulating UA, CRE, and BUN. The effects of stigmasterol 3-O-beta-D-glucopyranoside and 3 β -acetoxyatractylone on hyperuricemia have not been reported, but their derivatives can affect uric acid production and metabolism and have been shown in multiple studies to significantly alleviate inflammation and inhibit cell apoptosis.^{31–33} Therefore, they may have significant roles in inhibiting the development of hyperuricemia complications. The experiment confirmed that DED can significantly reverse the elevation of pro-inflammatory cytokines in renal tissue and inhibit cell apoptosis, indicating that the renal protective effect of DED may be due to its anti-inflammatory and anti-apoptotic effects, which is similar to previous studies.³⁴

In clinical practice, first-line drugs for reducing uric acid are mostly achieved by inhibiting XOD, but there are many adverse reactions, such as headaches, liver function damage, and allergic reactions.² The results of this experiment show that DED is similar to Western medicine and can effectively inhibit XOD activity. However, network pharmacology has found that XOD is only one of the numerous targets of DED and may even produce a small part of the effect. This experiment found that the active ingredients in network pharmacological analysis and molecular docking are well matched with multiple functional targets. The results showed that DED has a significant effect on renal inflammation and apoptosis by binding to multiple targets, such as IL6, TNF, CCL2, VEGFA, MAPK3, IL1B, CASP3, PPARG, CAT, and IL10, suggesting that it may regulate the AGE-RAGE and IL-17 double signaling pathway.^{6,35,36} The experimental results also confirm this viewpoint that DED can significantly inhibit the activation of the AGE-RAGE and IL-17 double signaling pathway. Compared to a single target, this multitarget combination may have a significant improvement effect on adverse drug reactions, making it possible

to combine DED with clinical hyperuricemia drugs.³⁷ DED can improve the clinical symptoms of hyperuricemia by reducing serum UA, CRE, and BUN and protecting against kidney damage. Research shows that BBR will present varying degrees of gastrointestinal damage,³⁸ while DED shows no side effects. Therefore, DED and BBR have similar effects and fewer side effects than hyperuricemia. To the best of our knowledge, this is the first study to determine the mechanism of DED in treating hyperuricemia. Through network pharmacology and molecular docking technology, this study determined the key mechanism by which DED alleviates hyperuricemia, but the side effects caused by the long-term use of traditional Chinese medicine prescriptions still need further research.³⁹ However, our research has some limitations. Although molecular docking is only a prediction of the relationship between DED and hyperuricemia targets, more experimental evidence is needed to determine whether there is a direct interaction between DED and hyperuricemia targets. In addition, our research on signaling pathways still needs to be validated by adding specific antagonists and inhibitors to fully explain the cell experiments.

Conclusion

DED significantly reduced the levels of serum UA, CRE and BUN and alleviated the kidney damage caused by hyperuricemia. Through network pharmacology and molecular docking analyses, we experimentally verified that DED can improve hyperuricemia by regulating the AGE-RAGE and IL-17 signaling pathways, which provides a new approach for the clinical treatment and prevention of hyperuricemia. This study provides a new theoretical basis for the drug development of DED in the treatment of hyperuricemia.

Data Sharing Statement

The data that supports the findings of this study are available on request from the corresponding author upon reasonable request.

Ethics Statement

The study was reviewed and approved by the Ethics Committee of The General Hospital of Western Theater Command (Approval No. 2022EC2-007).

Acknowledgments

We would like to show sincere appreciation to the reviewers for critical comments on this article.

Author Contributions

All authors made a significant contribution to the work reported, whether that is in the conception, study design, execution, acquisition of data, analysis and interpretation, or in all these areas; took part in drafting, revising or critically reviewing the article; gave final approval of the version to be published; have agreed on the journal to which the article has been submitted; and agree to be accountable for all aspects of the work.

Funding

This study was supported by General project of Sichuan Provincial Administration of Traditional Chinese Medicine (No.2021MS505), General Project of Sichuan Natural Science Foundation (No.2022NSFSC0738), Hospital Management research of Western Theater General Hospital (No.2021-XZYG-C16).

Disclosure

The authors report no conflicts of interest in this work.

References

1. Fathallah-Shaykh SA, Cramer MT. Uric acid and the kidney. *Pediatric Nephrology*. 2014;29(6):999–1008. doi:10.1007/s00467-013-2549-x
2. Becker MA, Schumacher HR, Wortmann RL, et al. Febuxostat compared with allopurinol in patients with hyperuricemia and gout. *N Engl J Med*. 2005;353(23):2450–2461. doi:10.1056/NEJMoa050373

3. Hou C, Sha W, Xu Z, et al. Culture and establishment of self-renewing human liver 3D organoids with high uric acid for screening antihyperuricemic functional compounds. *Food Chem.* 2022;374:131634. doi:10.1016/j.foodchem.2021.131634
4. Isaka Y, Takabatake Y, Takahashi A, et al. Hyperuricemia-induced inflammasome and kidney diseases. *Nephrol Dial Transplant.* 2016;31(6):890–896. doi:10.1093/ndt/gfv024
5. Yang L, Wang B, Ma L, et al. Traditional Chinese herbs and natural products in hyperuricemia-induced chronic kidney disease. *Front Pharmacol.* 2022;13:971032. doi:10.3389/fphar.2022.971032
6. Amatjan M, Li N, He P, et al. A novel approach based on gut microbiota analysis and network pharmacology to explain the mechanisms of action of cichorium intybus L. formula in the improvement of hyperuricemic nephropathy in rats. *Drug Des Devel Ther.* 2023;17:107–128. doi:10.2147/DDDT.S389811
7. Chen Y, Li C, Duan S, et al. Curcumin attenuates potassium oxonate-induced hyperuricemia and kidney inflammation in mice. *Biomed Pharmacother.* 2019;118:109195. doi:10.1016/j.biopha.2019.109195
8. Qian X, Jiang Y, Luo Y, et al. The Anti-hyperuricemia and anti-inflammatory effects of atracylodes macrocephala in hyperuricemia and gouty arthritis rat models. *Comb Chem High Throughput Screen.* 2023;26(5):950–964. doi:10.2174/1386207325666220603101540
9. Zhao M, Zhu D, Sun-Waterhouse D, et al. In vitro and in vivo studies on adlay-derived seed extracts: phenolic profiles, antioxidant activities, serum uric acid suppression, and xanthine oxidase inhibitory effects. *J Agric Food Chem.* 2014;62(31):7771–7778. doi:10.1021/jf501952e
10. Zhu L, Dong Y, Na S, et al. Saponins extracted from Dioscorea collettii rhizomes regulate the expression of urate transporters in chronic hyperuricemia rats. *Biomed Pharmacother.* 2017;93:88–94. doi:10.1016/j.biopha.2017.06.022
11. Liu L, Jiang S, Liu X, et al. Inflammatory response and oxidative stress as mechanism of reducing hyperuricemia of gardenia jasminoides-poria cocos with network pharmacology. *Oxid Med Cell Longev.* 2021;2021:8031319. doi:10.1155/2021/8031319
12. Linani A, Serseg T, Benarous K, et al. Cupressus sempervirens L. flavonoids as potent inhibitors to xanthine oxidase: in vitro, molecular docking, ADMET and PASS studies. *J Biomol Struct Dyn.* 2022;1–14. doi:10.1080/07391102.2022.2114943
13. Yang Y, Hua Y, Chen W, et al. Therapeutic targets and pharmacological mechanisms of Coptidis Rhizoma against ulcerative colitis: findings of system pharmacology and bioinformatics analysis. *Front Pharmacol.* 2022;13:1037856. doi:10.3389/fphar.2022.1037856
14. Xie W, Yang H, Guo C, et al. Integrated network pharmacology and experimental validation approach to investigate the mechanisms of stigmaterol in the treatment of rheumatoid arthritis. *Drug Des Devel Ther.* 2023;17:691–706. doi:10.2147/DDDT.S387570
15. Xia T, Liang X, Liu CS, et al. Network pharmacology integrated with transcriptomics analysis reveals ermiao wan alleviates atopic dermatitis via suppressing MAPK and activating the EGFR/AKT signaling. *Drug Des Devel Ther.* 2022;16:4325–4341. doi:10.2147/DDDT.S384927
16. Liu T, Gao H, Zhang Y, et al. Apigenin ameliorates hyperuricemia and renal injury through regulation of uric acid metabolism and JAK2/STAT3 signaling pathway. *Pharmaceuticals.* 2022;15(11):1442. doi:10.3390/ph15111442
17. Nogales C, Mamdouh ZM, List M, et al. Network pharmacology: curing causal mechanisms instead of treating symptoms. *Trends Pharmacol Sci.* 2022;43(2):136–150. doi:10.1016/j.tips.2021.11.004
18. Vargas-Santos AB, Neogi T. Management of Gout and Hyperuricemia in CKD. *Am J Kidney Dis.* 2017;70(3):422–439. doi:10.1053/ajkd.2017.01.055
19. Liang G, Nie Y, Chang Y, et al. Protective effects of Rhizoma smilacis glabrae extracts on potassium oxonate- and monosodium urate-induced hyperuricemia and gout in mice. *Phytomedicine.* 2019;59:152772. doi:10.1016/j.phymed.2018.11.032
20. Liu D, Yan J, Guo M, et al. Effect of methotrexate combined with Sanhuang Yilong decoction on serum and synovial fluid aquaporin levels in rheumatoid arthritis dampness-heat blockage syndrome. *J Tradit Chin Med.* 2018;38(4):618–624.
21. Yang M, Guo MY, Luo Y, et al. Effect of Artemisia annua extract on treating active rheumatoid arthritis: a randomized controlled trial. *Chin J Integr Med.* 2017;23(7):496–503. doi:10.1007/s11655-016-2650-7
22. Wang C, Zhou J, Wang S, et al. Guanxinging injection alleviates fibrosis in heart failure mice and regulates SLC7A11/GPX4 axis. *J Ethnopharmacol.* 2023;310:116367. doi:10.1016/j.jep.2023.116367
23. Chen Y, Jin S, Teng X, et al. Hydrogen sulfide attenuates LPS-induced acute kidney injury by inhibiting inflammation and oxidative stress. *Oxid Med Cell Longev.* 2018;2018:6717212. doi:10.1155/2018/6717212
24. Geng YH, Yan JH, Han L, et al. Potential molecular mechanisms of Ermiao san in the treatment of hyperuricemia and gout based on network pharmacology with molecular docking. *Medicine.* 2022;101(37):e30525. doi:10.1097/MD.00000000000030525
25. Song SH, Park DH, Bae MS, et al. Ethanol extract of cudrania tricuspidata leaf ameliorates hyperuricemia in mice via inhibition of hepatic and serum xanthine oxidase activity. *Evid Based Complement Alternat Med.* 2018;2018:8037925. doi:10.1155/2018/8037925
26. Ferraz-Filha ZS, Michel Araújo MC, Ferrari FC, et al. Tabebuia roseoalba: in vivo hypouricemic and anti-inflammatory effects of its ethanolic extract and constituents. *Planta Med.* 2016;82(16):1395–1402. doi:10.1055/s-0042-105878
27. Bao R, Wang W, Chen B, et al. Dioscin ameliorates hyperuricemia-induced atherosclerosis by modulating of cholesterol metabolism through FXR-signaling pathway. *Nutrients.* 2022;14(9):1983. doi:10.3390/nu14091983
28. Yang B, Xin M, Liang S, et al. Naringenin ameliorates hyperuricemia by regulating renal uric acid excretion via the PI3K/AKT signaling pathway and renal inflammation through the NF-κB signaling pathway. *J Agric Food Chem.* 2023;71(3):1434–1446. doi:10.1021/acs.jafc.2c01513
29. Wang M, Zhao J, Zhang N, et al. Astilbin improves potassium oxonate-induced hyperuricemia and kidney injury through regulating oxidative stress and inflammation response in mice. *Biomed Pharmacother.* 2016;83:975–988. doi:10.1016/j.biopha.2016.07.025
30. Schloss J, Ryan K, Steel A. Corrigendum to A randomised, double-blind, placebo-controlled clinical trial found that a novel herbal formula UROX[®] BEDTIME BUDDY assisted children for the treatment of nocturnal enuresis. *Phytomedicine.* 2022;99:153992. doi:10.1016/j.phymed.2022.153992
31. Yao J, He H, Xue J, et al. Mori ramulus (Chin.Ph.)-The dried twigs of morus alba L./part 1: discovery of two novel coumarin glycosides from the anti-hyperuricemic ethanol extract. *Molecules.* 2019;24(3):629. doi:10.3390/molecules24030629
32. Lee YS, Kim SH, Yuk HJ, et al. Tetragonia tetragonoides (Pall.) Kuntze (New Zealand Spinach) prevents obesity and hyperuricemia in high-fat diet-induced obese mice. *Nutrients.* 2018;10(8):1087. doi:10.3390/nu10081087
33. Ahmad NS, Farman M, Najmi MH, et al. Pharmacological basis for use of Pistacia integerrima leaves in hyperuricemia and gout. *J Ethnopharmacol.* 2008;117(3):478–482. doi:10.1016/j.jep.2008.02.031
34. Hassanein EHM, Mohamed WR, Ahmed OS, et al. The role of inflammation in cadmium nephrotoxicity: NF-κB comes into view. *Life Sci.* 2022;308:120971. doi:10.1016/j.lfs.2022.120971

35. Qian Y, Yin J, Ni J, et al. A network pharmacology method combined with molecular docking verification to explore the therapeutic mechanisms underlying simiao pill herbal medicine against hyperuricemia. *Biomed Res Int.* 2023;2023:2507683. doi:10.1155/2023/2507683
36. Huang J, Lin Z, Wang Y, et al. Wuling san based on network pharmacology and in vivo evidence against hyperuricemia via improving oxidative stress and inhibiting inflammation. *Drug Des Devel Ther.* 2023;17:675–690. doi:10.2147/DDDT.S398625
37. Liu H, Peng S, Yuan H, et al. Chinese herbal medicine combined with western medicine for the treatment of type 2 diabetes mellitus with hyperuricemia: a systematic review and meta-analysis. *Front Pharmacol.* 2023;14:1102513. doi:10.3389/fphar.2023.1102513
38. Heel RC, Brogden RN, Speight TM, Avery GS. Benzbromarone: a review of its pharmacological properties and therapeutic use in gout and hyperuricaemia. *Drugs.* 1977;14(5):349–366. doi:10.2165/00003495-197714050-00002
39. Chen D, Li Q, Zhang H, et al. Traditional Chinese medicine for hypertrophic scars-A review of the therapeutic methods and potential effects. *Front Pharmacol.* 2022;13:1025602. doi:10.3389/fphar.2022.1025602

Drug Design, Development and Therapy

Dovepress

Publish your work in this journal

Drug Design, Development and Therapy is an international, peer-reviewed open-access journal that spans the spectrum of drug design and development through to clinical applications. Clinical outcomes, patient safety, and programs for the development and effective, safe, and sustained use of medicines are a feature of the journal, which has also been accepted for indexing on PubMed Central. The manuscript management system is completely online and includes a very quick and fair peer-review system, which is all easy to use. Visit <http://www.dovepress.com/testimonials.php> to read real quotes from published authors.

Submit your manuscript here: <https://www.dovepress.com/drug-design-development-and-therapy-journal>